Accepted Manuscript

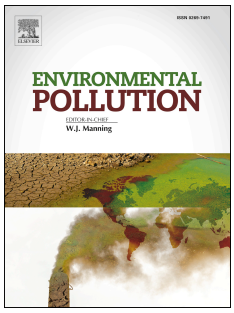

Subcellular distributions of trace elements (Cd, Pb, As, Hg, Se) in the livers of Alaskan yelloweye rockfish (*Sebastes ruberrimus*)

Benjamin D. Barst, Maikel Rosabal, Paul E. Drevnick, Peter G.C. Campbell, Niladri Basu

PII: S0269-7491(18)30204-5

DOI: 10.1016/j.envpol.2018.06.077

Reference: ENPO 11274

To appear in: *Environmental Pollution*

Received Date: 15 January 2018

Revised Date: 29 May 2018

Accepted Date: 22 June 2018

Please cite this article as: Barst, B.D., Rosabal, M., Drevnick, P.E., Campbell, P.G.C., Basu, N., Subcellular distributions of trace elements (Cd, Pb, As, Hg, Se) in the livers of Alaskan yelloweye rockfish (*Sebastes ruberrimus*), *Environmental Pollution* (2018), doi: 10.1016/j.envpol.2018.06.077.

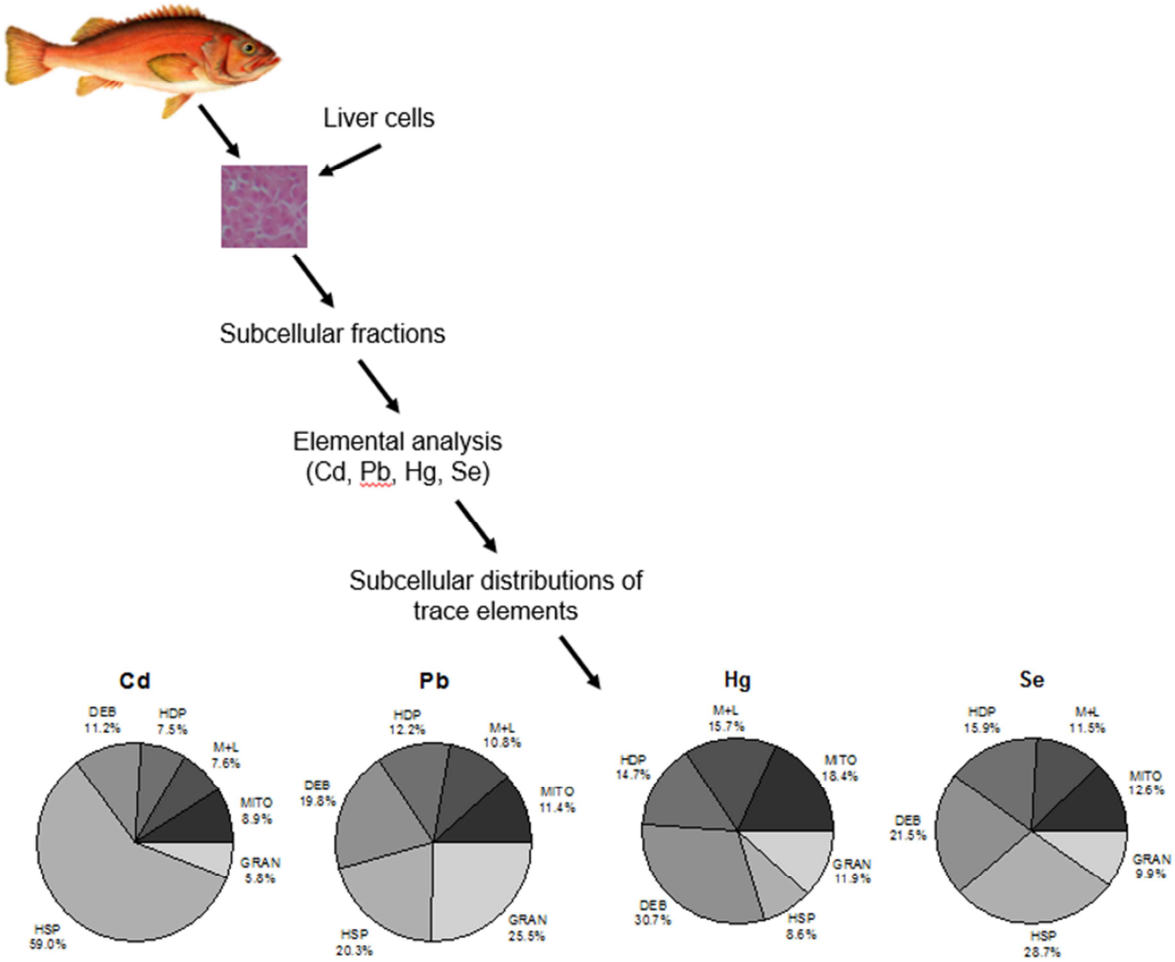
Liver cells
Subcellular fractions
Elemental analysis
(Cd, Pb, Hg, Se)
Subcellular distributions of
trace elements
Cd
DEB 11.2%
HDP 7.5%
M+L 7.6%
MITO 8.9%
GRAN 5.6%
HSP 59.0%
Pb
HDP 12.2%
M+L 10.8%
MITO 11.4%
GRAN 25.5%
HSP 20.3%
DEB 19.8%
Hg
M+L 15.7%
MITO 18.4%
GRAN 11.9%
HSP 8.6%
DEB 30.7%
HDP 14.7%
Se
HDP 15.9%
M+L 11.5%
MITO 12.6%
GRAN 9.9%
HSP 28.7%
DEB 21.5%

Subcellular distributions of trace elements (Cd, Pb, As, Hg, Se) in the livers of Alaskan yelloweye rockfish (*Sebastes ruberrimus)*

Benjamin D. Barst[a,b,*], Maikel Rosabal[c], Paul E. Drevnick[a,d], Peter G.C. Campbell[a], and Niladri Basu[b]

[a] Institut national de la recherche scientifique, Centre Eau Terre et Environnement (INRS-ETE), 490 de la Couronne, Québec, QC, Canada G1K 9A9

[b] Faculty of Agricultural and Environmental Sciences, McGill University, Montreal, QC, Canada, H9X 3V9

[c] Département des sciences biologiques, Université du Québec à Montréal (UQÀM), Montréal, QC, Canada, H2X 1Y4

[d] Environmental Monitoring and Science Division, Alberta Environment and Parks, Calgary, AB Canada, T2E 7L7

[*]Corresponding author: Tel.: +1 514 216 6019; benjamin.barst@mcgill.ca

Abstract

Yelloweye rockfish (*Sebastes ruberrimus*) is an extremely long-lived species (up to ~120 years) of fish, which inhabits the coastal waters of Alaska. Due to their long lifespans, yelloweye are known to accumulate high levels of mercury, and potentially other trace elements, in their tissues. Relatively little is known about the subcellular distribution of trace elements in the tissues of yelloweye rockfish; such information can provide important insights into detoxification/toxicity mechanisms at the subcellular level. To address this, we collected yelloweye rockfish (n=8) from the eastern coast of Prince of Wales Island, Alaska in 2014. We determined the subcellular partitioning of trace elements (cadmium (Cd), lead (Pb), arsenic (As), total mercury (Hg), and selenium (Se)) in yelloweye livers with a partitioning procedure designed to separate liver cells into putative metal-sensitive fractions (cytosolic enzymes, organelles) and detoxified metal fractions (metallothionein or metallothionein-like proteins and peptides, granule-like structures) using differential centrifugation, NaOH digestion, and heat denaturation steps. The resulting fractions were then analyzed for total Hg with a direct Hg analyzer and for trace element concentrations by inductively coupled plasma-mass spectrometry (ICP-MS). For Cd, Pb, and As, the greatest contributions were found in the detoxified fractions, whereas the majority of total Hg was found in sensitive fractions. Selenium, an essential trace element, was distributed to a similar degree between the sensitive and detoxified compartments. Results indicate that although yelloweye sequestered and immobilized potentially toxic metals in detoxified fractions, the extent of binding differed among metals and followed the order: Cd > As > Pb > Hg. In yelloweye rockfish livers, the accumulation of non-essential elements at sensitive sites could lead to deleterious effects at the subcellular level, which should be evaluated in future studies.

Keywords: subcellular partitioning; trace elements; mercury; detoxification; yelloweye rockfish; Alaska

Capsule: Subcellular partitioning of yelloweye rockfish livers aids in understanding detoxification of trace elements

1. Introduction

Yelloweye rockfish (YR; *Sebastes ruberrimus*) are one of the largest species of rockfish inhabiting the marine waters of western North America, where their range extends from the Aleutian Islands to the Baja Peninsula (Love et al., 2002). As their name would suggest, they often pass most their considerable lifespans (up to ~120 years) near steep rock piles on the ocean floor. Their long lifespans, large body size, and late age at sexual maturity render them particularly susceptible to both recreational and commercial fishing pressures. Currently, YR are listed as threatened in the Puget Sound-Georgia Basin of the United States (NMFS, 2010) and as a species of special concern in Canada (COSEWIC, 2009). In addition to overfishing, YR may be at risk from exposure to contaminants, as their tissues are known to contain elevated concentrations of mercury (Hg) (Barst et al., 2015). For example, total Hg concentrations in the edible muscle tissue of YR often exceed 0.5 $\mu g\ g^{-1}$ wet weight (ww), the level at which sublethal effects in fish are likely to occur (Sandheinrich and Wiener, 2011).

Despite reports of contamination of YR tissues, the associated health effects have remained largely unexplored, as is the case for many wild species of fish. An exception, by Barst et al. (2015), compared concentrations of essential (selenium (Se), copper (Cu), zinc (Zn)) and non-essential trace elements (nickel (Ni), cadmium (Cd), mercury (Hg)) with the relative areas of melano-macrophage aggregates (MA) in YR livers. Melano-macrophage aggregates are collections of immune cells that serve to store and process the products of cell breakdown, and are considered a general biomarker of contaminant exposure in fish (Wolke, 1992). An increase in MA area is often interpreted as an indication of tissue damage. In YR livers, the relative areas of MA increased with increasing hepatic concentrations of Hg, Se, Cd, and Cu, and these elements tended to be more concentrated in MA than the surrounding tissues. The accumulation of non-essential metals in the MA of fish may indicate increased cell turnover due to metals exposure. Interestingly, Hg and Se accumulated in MA to a similar extent, suggesting that the two were present as a mercury selenide complex (Barst et al., 2015). The biological interaction of Hg and Se has been well documented (Khan and Wang, 2009; Wang et al., 2012), and HgSe is widely regarded as a non-bioavailable end-product of Hg detoxification in the organs of different species (Korbas

et al., 2010; Palmisano et al., 1995). Furthermore, Se may also protect against Cd toxicity in wild fishes (Ponton et al., 2016).

With this in mind, the determination of the subcellular distributions of trace elements may be useful in determining the likelihood for toxic effects in the livers of YR, and may provide an overall greater understanding of trace element partitioning in wild fish. Subcellular partitioning allows for the distinction between metal-binding to potentially sensitive target molecules (e.g., cytosolic enzymes) and organelles (e.g., mitochondria), where the binding of non-essential metals may lead to negative effects, and metal accumulation in detoxified metal fractions (e.g., heat-stable proteins and metal-rich granules), which may minimize toxic effects (Campbell and Hare, 2009; Wallace et al., 2003). In this context, we determined the subcellular partitioning of Cd, Pb, As, total Hg, and Se in order to further our understanding of the internal handling of these elements in the livers of YR collected in southeast Alaska, USA. A subcellular partitioning procedure using differential centrifugation, NaOH digestion, and heat denaturation steps was used to separate liver cells into operationally-defined metal-sensitive fractions (mitochondria, microsomes and lysosomes, and heat-denatured proteins) and detoxified-metal fractions (heat-stable proteins and metal-rich granules). Following separation, trace elements were measured in each fraction to determine the degree to which YR are able to detoxify non-essential elements effectively, and to identify non-essential elements of concern for risk assessment.

2. Material and Methods

2.1. Sampling site and fish collection

In July 2014, adult YR (n=8; Table 1) were collected from Ernest Sound (55°51'59"N, 132°12'46"W) located near Prince of Wales Island, Alaska. The sampling location was selected based on metal concentrations presented in Barst et al. (2015). Fish were caught using rod and reel and were euthanized immediately after capture. Fish lengths (cm) and weights (g) were recorded. Livers were removed, divided for subcellular and bulk tissue analyses, and immediately frozen and maintained at -25 °C in the

field (2 weeks). After returning from the field, frozen samples were kept at -80 °C (at INRS-ETE) until processing.

2.2. Subcellular partitioning procedure

Yelloweye rockfish liver samples were separated into subcellular fractions (Figure S1, Supplementary Information): nuclei and debris; granule-like; mitochondria; microsomes and lysosomes; heat-denatured proteins (HDP), which include cytosolic enzymes; and heat-stable proteins and peptides (HSP), such as metallothionein (MT) and glutathione (GSH). The subcellular partitioning procedure was adapted from previous protocols described by Wallace et al. (2003) and Giguère et al. (2006). The effectiveness of the procedure at isolating subcellular fractions has been assessed previously by using enzymes as molecular markers for specific fractions or organelles (Rosabal et al., 2015). We stress that these fractions are operationally-defined in nature. Furthermore, the designation "microsomes" refers to structures which form a pellet at a given centrifugation speed, rather than structures found within cells. The details of the partitioning procedure were based on previously published methods (Rosabal et al. 2012; Rosabal et al. 2014) and can be found in the Supplementary Information.

2.3. Trace element measurements and quality control

The preparation of tissue homogenates and subcellular fractions is provided in the Supplementary Information. Total Cd, Pb, As, and Se concentrations in all subcellular fractions were measured using an inductively coupled plasma-mass spectrometer (ICP-MS; Thermo Elemental X Series, Winsford, England, United Kingdom). Samples of similar weight of a certified reference material (TORT-2, lobster hepatopancreas, National Research Council of Canada, NRCC, Halifax, Nova Scotia, Canada) were subjected to the same digestion procedure and analyzed concurrently with YR fractions. The recovery of elements from TORT-2 (n = 2) was 91 ± 0.11% for Cd, 79 ± 4.6% for Pb, 106 ± 0.1% for As, and 90 ± 5.6% for Se. The relative percent difference (RPD) between duplicate samples for Cd, Pb, As, and Se were 0.1%, 8.3%, 0.07%, and 8.8%, respectively.

Total Hg measurements were carried out using a direct mercury analyzer (DMA-80, Milestone Inc., Monroe, CT), which uses thermal decomposition, amalgamation, and atomic absorption spectrophotometry according to the U.S. Environmental Protection Agency (US EPA) Method 7473 (US EPA, 2007). Quality assurance consisted of analysis of certified reference materials MESS-3 (marine sediments; n=7) and DOLT-4 (dogfish liver; n=6), National Research Council of Canada, NRCC, Halifax, Nova Scotia, Canada). Mean percent recovery of total Hg from MESS-3 was 97 ± 1.4 % and the relative standard deviation (RSD) was 1.5 %. Mean percent recovery of total Hg from DOLT-4 was 98 ± 3.8 % and the RSD was 3.9 %. Mass balances for Cd, Pb, As, Hg, and Se are reported in the Supplementary Information.

2.4. Total mercury measurements in bulk muscle tissue

Freeze-dried samples of bulk muscle tissues were analyzed for total Hg using a direct Hg analyzer (DMA-80, Milestone Inc., Monroe, CT). Quality assurance consisted of the analysis of certified reference materials (DORM-4: fish protein, National Research Council Canada, Ottawa, Canada) and duplicate samples. The recovery of total Hg from DORM-4 was 96 % (n=2) and the RPD between duplicate samples was 0.80 % (n=2). In order to compare Hg concentrations to published values, wet weight concentrations in YR muscle samples were estimated by assuming a moisture content of 80%, which is consistent with a previous study with YR (Barst et al. 2015).

2.5. Data analyses

The contribution of each subcellular fraction relative to the total element burden was estimated as a ratio defined by the element burden in a given fraction divided by the sum of element burdens in all fractions, multiplied by 100 to give results as percentages (%). Element concentrations in all subcellular fractions are expressed as total element burden (nmol) divided by the liver dry weight (g, dw). Liver dry weights were determined by weighing subsamples of liver tissue before and after freeze-drying. All numerical data are represented by means ± standard deviations (SD), unless otherwise noted. Relationships among variables (trace element concentrations and relative contributions) were initially examined in bivariate

scatterplots and tested by simple correlation (Pearson r) after checking the assumption of normality (Shapiro–Wilk test) and testing for outliers (Grubb's test). Percentage data (relative contribution of each subcellular fraction to the total metal burden) were arcsine transformed. If non-normality persisted, a non-parametric correlation was reported (Spearman r). When bivariate plots indicated a possible linear relationship, simple regression models were tested using the ordinary least-squares equation when the necessary assumptions (normality and homoscedasticity of residuals) were satisfied. The Shapiro–Wilk test was used to verify the normality of distributions of the regression residuals. The Breusch-Pagan test was used to test the homoscedasticity of the regression residuals. For the trace elements (Pb, Hg, and Se) that showed significant increases in more than one subcellular fraction within either the sensitive or detoxified compartments, the slopes of the linear regressions were compared using analysis of covariance (ANCOVA) in order to compare the responses along the bioaccumulation gradient. Note that a parametric assessment of covariance was preferred given that the residuals of the linear regressions were normally distributed. To explore similarities (or differences) in how hepatic trace metals were partitioned between both subcellular compartments (detoxified and metal-sensitive), we performed two separate PCA analyses that combined data into two-component models and explained 80 - 86% of the variation. The first PCA used trace element concentrations in combined sensitive fractions, and the second used trace element concentrations in combined detoxified fractions. An $\alpha < 0.05$ was used as the threshold of significance for all statistical tests. All statistical analyses were performed with JMP Pro 13 Statistical Analysis Software (SAS Institute, Cary, NC, USA).

3. Results

3.1. Trace element accumulation in yelloweye rockfish liver

Trace element concentrations in YR livers, as well as YR lengths and weights, are reported in Table 1. Liver trace element concentrations did not vary significantly with the length or weight of the fish. The ratio of maximum to minimum trace element concentrations ($[M]_{max}/[M]_{min}$) in YR livers was greatest for Cd (9.0), followed by Pb (4.7), Hg (4.1), Se (3.0), and As (2.9). Total Hg concentrations (µg g^{-1} ww) are also reported for YR muscle in Table 1. Note that the simplest explanation for the variations in $[M]_{max}/[M]_{min}$ ratios is that the uptake : elimination ratio along the sampling gradient differs for the measured trace elements (Luoma and Rainbow, 2005). Muscle total Hg concentrations ranged from 0.3 to 1.4 µg g^{-1} ww. Muscle total Hg concentrations are reported in µg g^{-1} ww so that concentrations are easily comparable to established toxicity thresholds (Dillon et al., 2010; Sandheinrich and Wiener, 2011). Note that we did not determine the ages of the rockfish in the present study, however Barst et al. (2015) reported ages of YR, collected from the same sampling location and of comparable size, ranging from 16 to 119 years.

3.2. Trace element subcellular partitioning

We plotted trace element concentrations in whole liver against concentrations (nmol g^{-1} dw) in potentially sensitive (mitochondria, microsomes and lysosomes, and heat-denatured protein fractions) and detoxified subcellular fractions (heat-stable proteins and granule-like fractions), in order to explore potential changes in partitioning with increasing element concentrations in whole liver (Figures 1 and 3). We also investigated possible relationships between the percentage of each trace element found in the various subcellular fractions relative to the total trace element concentrations (nmol g^{-1} dw) (Figures S2 and S3, Supplementary Information). If the percentages of trace elements in each fraction did not change significantly along the bioaccumulation gradient, then data for all fish were combined to produce mean percent contributions for the various subcellular fractions per element (Figures 2 and 4). As the toxicological significance of trace element accumulation in the nuclei and debris fraction is ambiguous,

this fraction has been generally ignored in the ecotoxicological literature (Campbell and Hare, 2009). However, as this fraction tends to accumulate unbroken cells, it may indicate the efficacy of the homogenization step; a low and constant proportion of the trace-element in question found in the nuclei and debris suggests an efficient and precise homogenization. In the following sections, we present the results of the subcellular partitioning procedure for each of the studied trace elements.

3.3. Cd (cadmium)

There were no significant relationships between total hepatic Cd and concentrations in any of the subcellular fractions in the potentially-sensitive compartment (Figure 1A). However, the concentration of Cd in the HSP fraction increased significantly as the total hepatic Cd concentration increased ($r^2 = 0.71$; slope = 0.75; $P = 0.02$; Figure 1B). There were no significant relationships between the relative contributions of the fractions and total hepatic Cd (Figures S2A and S2B, Supplementary Information). When data from all fish were combined, the majority of Cd was associated with the detoxified compartment (65%), with the sensitive compartment contributing only 25%. The HSP fraction contributed the majority of the Cd in the detoxified compartment (59%), with only a minor contribution attributed to the granule-like fraction (6%). In the potentially-sensitive compartment, Cd was more or less equally distributed among the mitochondria (9%), the microsomes and lysosomes (8%), and the HDP (8%) fractions (Figure 2).

3.4. Pb (lead)

Note that total Pb concentrations (< 1 nmol g^{-1} dry wt) in the livers of YR were much lower than molar concentrations of Cd, As, Hg, and Se. Nevertheless, the Pb concentrations increased in both the mitochondria ($r^2 = 0.75$; slope = 0.11 ± 0.03; $P = 0.006$) and HDP ($r^2 = 0.74$; slope = 0.091 ± 0.02; $P = 0.006$) fractions with increasing Pb concentration in whole liver to a similar extent, as evidenced by the similar slopes of the two regressions ($P = 0.82$) (Figure 1C). The concentration of Pb increased significantly in both the HSP ($r^2 = 0.85$; slope = 0.24 ± 0.04; $P = 0.001$) and granule-like ($r^2 = 0.87$; slope = 0.31 ± 0.06; $P = 0.0007$) fractions along the bioaccumulation gradient (Figure 1D). The rates of

increase in Pb concentration within the two detoxified fractions were not significantly different from one another (P = 0.98). When comparing sensitive and detoxified fractions, the slope of the line representing the HDP fraction was significantly lower than the slopes for both the HSP (P = 0.04) and granule-like fractions (P = 0.04) (Figure 1C and 1D). The total hepatic Pb concentration was not significantly correlated with the relative contribution of Pb in any of the subcellular fractions (Figures S2C and S2D, Supplementary Information). When combining data from all fish, the mean relative contribution of the detoxified compartment was 46%, of which the majority was contributed by the granule-like fraction (26%). The potentially-sensitive compartment contributed only 35% of the total Pb. In the potentially-sensitive compartment, Pb was distributed similarly among the HDP (12%), mitochondria (11%), and the microsomes and lysosomes (11%) fractions (Figure 2).

3.5. As (arsenic)

Though the concentration of As increased in the mitochondria fraction along the bioaccumulation gradient (r^2 = 0.57; P = 0.03), the rate of increase began to plateau at higher total hepatic As concentrations (Figure 1E). Conversely, there were no significant relationships between total hepatic As and concentrations in either the HDP or microsomes and lysosomes fractions. The concentration of As in the HSP fraction increased significantly with increasing As in whole liver (r^2 = 0.84; slope = 0.86; P = 0.01) (Figure 1F). The relative contributions of As increased significantly in the HSP (r^2 = 0.60; P = 0.02), while decreasing in the microsomes and lysosomes (r^2 = 0.51; P = 0.046) along the bioaccumulation gradient (Figures S2E and S2F, Supplementary Information). Among all fish, the relative contributions of the HSP and granule-like fractions to the total hepatic As burden varied from 50% to 75% and 2% to 9%, respectively. The relative contributions of the mitochondria, microsomes and lysosomes, and HDP fractions varied from 7% to 14%, 4% and 10%, and 5% and 10%, respectively.

3.6. *Hg (mercury)*

As the concentration of total Hg increased in whole liver, the concentrations of total Hg increased in the mitochondria (r^2 = 0.86; slope = 0.25; P = 0.001), microsomes and lysosomes (r^2 = 0.91; slope = 0.17; P =

0.0002), HSP (r^2 = 0.58; slope = 0.04; *P* = 0.03), and granule-like fractions (r^2 = 0.64; slope = 0.07; *P* = 0.03) (Figures 3A and 3B). Within the sensitive compartment, the increase in total Hg in the mitochondria fraction was greater than in the microsomes and lysosomes fraction (*P* = 0.03). Conversely, within the detoxified compartment, total Hg increased in the HSP and granule-like fractions to a similar extent along the bioaccumulation gradient (*P* = 0.45). Total Hg increased in both the mitochondria and microsomes and lysosomes fractions to a greater extent than in the HSP or granule-like fractions ($P<0.05$). The relative contributions of the various subcellular fractions to total hepatic Hg did not vary significantly along the bioaccumulation gradient (Figures S3A and S3B, Supplementary Information). For all fish, the mean proportion of total Hg in the detoxified compartment was 21%, with about half being contributed by the granule-like fraction (12%). Discounting the nuclei and debris fraction, the majority of the total hepatic Hg burden was associated with the potentially-sensitive compartment (49%). Within this compartment, the contributions of the individual fractions decreased in the order mitochondria (18%) ≥ microsomes and lysosomes (16%) ≥ HDP (15%) (Figure 4).

3.7. Se (selenium)

Concentrations of Se increased significantly in all of the subcellular fractions, except for the granule-like fraction, as Se increased in whole liver. Within the potentially-sensitive compartment, the relation with total hepatic Se was tightest for HDP (r^2 = 0.95; slope = 0.16 ± 0.02; *P* = 0.0002) followed by mitochondria (r^2 = 0.90; slope = 0.16 ± 0.02; *P* = 0.0003), and microsomes and lysosomes (r^2 = 0.67; slope = 0.08 ± 0.02; *P* = 0.01) fractions, though there were no significant differences among the slopes of the regressions (Figure 3C). Within the detoxified compartment, Se increased significantly only in HSP (r^2 = 0.76; slope = 0.27; *P* = 0.0051) (Figure 3D). The increase in Se concentration in HSP was significantly greater than in the mitochondria (*P* = 0.04) or microsomes and lysosomes (*P* = 0.002) fractions. The relative contributions of the various subcellular fractions to the total hepatic Se concentration did not vary significantly as a function of the total hepatic Se concentration (Figures S3C and S3D, Supplementary Information). When data for all fish were combined, Se was associated with

potentially-sensitive and detoxified compartments similarly (40% and 39%, respectively). A larger percentage of Se was found in the HSP fraction (29%), than the granule-like fraction (10%). In the potentially-sensitive compartment, the relative contributions of Se were similar, decreasing in the order of the HDP fraction (16%) followed by mitochondria (13%), and microsomes and lysosomes (12%) (Figure 4).

4. Discussion

4.1. General considerations

The limited sample size in the present study was dictated by difficulties in sampling the Alaskan YR and the conservative catch limits enforced by the State of Alaska. Despite the small sample size, our results increase knowledge related to the internal handling of trace elements in wild fish. Our study is unique in that YR have an unusually long life span compared to other fish for which the subcellular partitioning of trace elements has been reported. Note too that most other studies in this area have been limited to 'traditional' metals such as Cd, Hg and Pb, whereas in the present study we have also included two metalloids, As and Se.

Numerous studies have applied subcellular partitioning procedures to determine the distribution of non-essential elements in the tissues of aquatic organisms (Giguère et al., 2006; Rosabal et al., 2015; Wang et al., 2016). These procedures provide insight into how aquatic organisms cope with non-essential metals and indicate whether toxicological effects are likely to occur. However, partitioning procedures are subject to potential problems which have been described in depth elsewhere (Campbell and Hare, 2009; Hinton et al., 1997). Subcellular fractions are operationally-defined, and accordingly the interpretation of partitioning results should be carried out with circumspection.

In this context, the terms "MT-like" or "granule-like" should be considered carefully. A previous study on *Chaoborus* larvae showed that not all metals measured in the HSP fraction are necessarily associated with MT or MTLP (Rosabal et al., 2016; Caron et al. 2018). This caveat is likely particularly important for As and Se, which tend to form covalent bonds with oxygen or reduced sulphur and may

exist as oxyanions or esters in the intracellular environment, rather than as chelated cations. Furthermore, the definitions of the "metal detoxified pool" and the "metal-sensitive pool" were designed for (soft) cationic metals, not for As (a metalloid that is reduced to and is largely present as As(III) in living cells) or Se. Moreover, the lumping of fractions into potentially-sensitive (mitochondria, HDP, microsomes and lysosomes fractions) and detoxified-metal compartments (HSP and granule-like), is likely an oversimplification (Campbell and Hare, 2009; Wallace et al., 2003). For example, microsomes cannot be separated effectively from lysosomes using the procedure in the present study, and this renders the interpretation of results more difficult. If a non-essential metal is primarily associated with lysosomes, then the metal has likely been detoxified. Conversely, the endoplasmic reticulum is a potential target for metal toxicity, and therefore, metals associated with these vesicles may cause deleterious effects. Previous studies have often grouped the microsome and lysosome fraction in the metal-sensitive compartment due to the important functions carried out by the endoplasmic reticulum, Golgi apparatus, and ribosomes in the liver. However, strict inclusion of this fraction in the sensitive compartment may not be appropriate for all metals. For instance, a recent study demonstrated, with electron energy loss spectrometry (EELS), that Hg accumulates in the hepatic lysosomes of wild yellow perch (*Perca flavescens*) (Müller et al., 2015). With this in mind, Hg (and potentially other trace elements) within the microsomes and lysosomes fraction may be associated with lysosomes to a greater extent than microsomes. As previously mentioned, the accumulation of non-essential metals in the nuclei and debris fraction is also difficult to interpret.

4.2. Cd (cadmium)

The high proportion of Cd associated with the HSP fraction suggests that Cd is largely detoxified by MT in YR livers, particularly for concentrations up to ~150 nmol g^{-1} dw. The lack of increasing trends between total hepatic Cd and the Cd concentration in sensitive fractions suggests this nonessential metal is largely kept under control in the livers of YR. Furthermore, the much lower Cd concentrations in sensitive fractions relative to that in HSP suggest effective detoxification. An interaction between HSP and Cd is consistent with the classification of Cd as a class B metal, which exhibits preferences for

reduced sulphur within cells (Mason and Jenkins, 1995). Elevated proportions of Cd were also found in the HSP fractions isolated from livers of wild American and European eels (Rosabal et al., 2015), as well as wild yellow perch (Giguère et al., 2006). Laboratory studies also indicate the importance of the HSP fraction in detoxifying Cd in fish. For example, Olsson and Hogstrand (1987) showed that Cd was associated with MT in rainbow trout livers following a 1-week aqueous exposure to ^{109}Cd (3-60 ng/L). Ng and Wood (2008) noted elevated proportions of Cd in fractions containing MT-like proteins isolated from the gut tissue of rainbow trout fed contaminated oligochaetes. Similarly, Zhang and Wang (2006) reported that the HSP fraction was the major storage compartment for Cd in the viscera of juvenile marine grunt fed brine shrimp previously exposed to aqueous ^{109}Cd. Together, these studies indicate that maintaining Cd in the HSP fraction is an important metal-handling strategy for fish species.

Though YR in the present study maintained the majority of Cd in the detoxified compartment, detoxification was not complete given the presence of some Cd at sensitive sites. In the sensitive compartment, isolated from whole zebrafish (*Danio rerio*) fed contaminated chironomids (153 – 288 µg g^{-1} dw), Cd was found mainly in the "organelles" fraction (including mitochondria and microsomes and lysosomes) followed by the HDP fraction (Béchard et al., 2008), which was similar to results for YR in the present study. Interestingly, the concentration of Cd did not increase significantly in sensitive fractions of YR livers along the bioaccumulation gradient, contrary to what was shown for wild yellow perch (Giguère et al., 2006) and wild American and European yellow eels (Rosabal et al., 2015). This may be due to the more modest Cd gradient in the present study ($[Cd]_{max}$: $[Cd]_{min}$ = 9.0) relative to the gradients reported by (Giguère et al., 2006) ($[Cd]_{max}$: $[Cd]_{min}$ = 14) and Rosabal et al. (2015) (American eels $[Cd]_{max}$: $[Cd]_{min}$ = 103 and European eels $[Cd]_{max}$: $[Cd]_{min}$ = 200). Moreover, the lack of significant relationships between Cd in sensitive fractions and Cd in whole liver may be a result of the variability in Cd concentrations. For example, two YR in the present study had total hepatic Cd concentrations of ~90 nmol g^{-1} dw, yet the Cd concentrations within the sensitive fractions of these individuals were quite different. This may indicate that individual YR can have less-(or more-)effective metal detoxification

systems than other fish in their population, a phenomenon that has been demonstrated previously for yellow perch sampled from metal-impacted lakes (Couture and Pyle, 2008).

Nevertheless, Cd was associated with sensitive subcellular sites within YR livers, and this could lead to negative health effects. Accumulation of Cd in mitochondria may affect functioning of this organelle, including an inhibition of citrate synthase, which has been documented for yellow perch livers collected from a highly contaminated lake in Canada (Couture and Rajotte, 2003). In a separate study with yellow perch, Ponton et al. (2016) noted that individuals suffering from oxidative stress had higher percentages of Cd, Cu, and Zn in potentially sensitive subcellular fractions, which may highlight the importance of maintaining these metals in detoxified fractions.

4.3. Pb (lead)

Within the detoxified compartment, Pb associated with the granule-like fraction to a slightly greater extent than with the HSP fraction. The preference for the granule-like fraction over the HSP fraction containing MT may be due to the fact that Pb, as a borderline metal, associates less readily with thiol groups than other “softer” metals, such as Cd and Ag (Mason and Jenkins, 1995). Nonetheless, the concentration of Pb increased in both the metal-rich granule and HSP fractions along the bioaccumulation gradient. Given the low Pb concentrations, the association of Pb with the HSP fraction may be an indirect response to Cd, which has consistently been shown to induce synthesis of MT. Following the induction of MT by Cd, MT is available to bind both Cd and other metals such as Pb. Alternatively, the association of Pb with the HSP fraction could be an indication of a detoxification response, although this seems unlikely given the very low concentrations of hepatic Pb. Much of the previous research involving the subcellular distribution of Pb has focused on invertebrates, with only a few studies reporting Pb partitioning in the tissues of fish. The distribution of Pb within the detoxified compartment of YR livers agrees well with the results of studies on invertebrates (Marigómez et al., 2002; Mason and Jenkins, 1995; Sánchez-Marín and Beiras, 2017; Wang et al., 2016) and other fish (Goto and Wallace, 2010; Rosabal et al., 2015), which show collectively that metal-rich granules are the primary binding pool within the detoxified

compartment. Contrary to these results, Dang et al. (2012) reported that the majority of Pb was found in the HSP fraction of intestinal cells of the marine grunt (*Terapon jarbua).*

Though Pb increased in detoxified fractions of YR liver, detoxification was incomplete given that Pb was also present in metal-sensitive fractions and increased along the bioaccumulation gradient. In terms of percentage, Pb was distributed similarly among the metal-sensitive fractions, only showing a slight preference for HDP. Consistent with our results, Rosabal et al. (2015) also reported increases of Pb in metal-sensitive fractions of yellow eels with increasing concentrations in whole liver. However, Pb did not increase in the metal-sensitive fractions of mummichogs (*Fundulus heteroclitus*) collected from metal-polluted salt marshes, though the two-fold bioaccumulation gradient of Pb was somewhat limited (Goto and Wallace, 2010). In YR, the association of Pb with metal-sensitive fractions may result in deleterious effects, in view of the ability Pb to replace other essential metals, such as Ca, within biological systems (Rogers et al., 2003). Furthermore, associations between Pb and mitochondria, enzymes, and microsomes would be expected to disrupt cellular processes. However, given the very low total hepatic Pb concentrations in the livers of YR in the present study, it is unlikely that this metal was of great toxicological concern to these fish.

4.4. As (arsenic)

Within the detoxified compartment of YR livers, As was primarily associated with the HSP fraction, containing MT. A steady increase of As in HSP suggests that this fraction may be involved in As detoxification within YR livers. To our knowledge, there are no previous studies on subcellular partitioning of As in the livers of rockfish species, though our results compare well with As partitioning in American and European yellow eels (*Anguilla rostrata* and *Anguilla anguilla*); like YR, both eel species maintained As in the HSP fraction, and to a lesser extent, in the metal-rich granule fraction (Rosabal et al., 2015). Similarly, in seabass (*Lateolabrax japonicas*) and seabream (*Pagrosomus major*) muscle, As was largely associated with the HSP fraction (He et al., 2010). These results are also consistent with a study on marine grunt (*Terapon jarbua*) exposed to dietary or aqueous As(III) and As(V) at environmentally-relevant concentrations for 10 d. In grunt muscle tissues, As accumulated

mainly in the HSP fraction, whereas less was associated with metal-rich granules (Zhang et al., 2012). Although As was associated with the HSP fraction there may not be a significant interaction between As and MT given the lower affinity this metalloid has for thiol functional groups.

In the metal-sensitive compartment, As was predominately associated with the mitochondria fraction, which is consistent with results from a previous study on American and European yellow eels (Rosabal et al., 2015). Our results differ slightly from the study by Rosabal et al. (2015) in that in eel livers, the microsomes and lysosomes fraction was a more important binding pool for As than the HDP fraction. In the present study, the microsomes and lysosomes and HDP fractions contributed roughly the same amount of As to the total As burden in YR livers. A study by Dang et al. (2012) noted binding of As in the "organelles" fraction (mitochondria and microsomes and lysosomes) of a polychaete worm (*Nereis diversicolor*) sampled from a contaminated estuary. In the same study, the contaminated worms were fed to fish (*Terapon jarbua*), which subsequently accumulated As in the hepatic "organelle" fraction. The combined results from these studies suggest that across species, organelles may be an important target for As at the subcellular level.

Along the As contamination gradient, we noted an increase in the relative contribution of As in the HSP fraction within YR livers, coupled with a decrease in the relative contribution of the microsomes and lysosomes fraction, suggesting an activation of detoxification mechanisms. Interestingly, the relative contributions of As in the mitochondria and HDP fractions increased with increasing As in whole liver until approximately 80 nmol g^{-1} dw, at which point the relative contribution of As in the fractions decreased along the bioaccumulation gradient (this was also the case for the microsomes and lysosomes fraction, though the increase and subsequent decrease in relative contribution of As was less pronounced, thus allowing for a significant linear trend to be fitted) (Figures S2E and S2F, Supplementary Information). The distributions of the relative contributions of As along the gradient suggest that detoxification of As became more effective above ~80 nmol g^{-1} dw in the livers of YR. This is similar to what Rosabal et al. (2012) noted for Cd in *Chaoborus*, i.e. a certain threshold of Cd was necessary to "turn on" detoxification mechanisms fully.

In the present study we did not determine As speciation in the livers of YR, though speciation of As is a major determinant of its toxicity (Watanabe and Hirano, 2013). Future work should focus on determining the oxidation state and methylation levels of As in wild fish at the subcellular level. Additionally, we highlight the need for subsequent work to identify the As-bearing molecules in the cytosol, specifically in the HSP fraction, which appears to be involved in As detoxification.

4.5. Hg (mercury)

Relatively few studies have focused on the subcellular distribution of Hg in fish liver (Araújo et al., 2015; Barst et al., 2016; Peng et al., 2016). Araújo et al. (2015) measured total Hg in subcellular fractions of the livers of wild mullets (*Liza aurata*), and found low contributions of Hg in the HSP and granule fractions, which the authors attributed to Hg concentrations below a physiological threshold to activate detoxification mechanisms. In Arctic char (*Salvelinus alpinus*) liver cells, Barst et al. (2016) reported that the HSP fraction was the primary binding pool for total Hg within the detoxified compartment, and less than 1% of the total Hg burden was found in the metal-rich granule fraction. Similarly, metal-rich granules played a less important role in the detoxification of methylmercury (MeHg) than MT-like proteins in the livers of rabbitfish (*Siganus canaliculatus*) (Peng et al., 2016). Results of the present study contrast with those from these earlier studies suggesting that the HSP fraction is more important than metal-rich granules in the detoxification of Hg in fish liver cells. A plausible explanation for the greater importance of the metal-rich granule fraction than the HSP fraction in sequestering Hg in the livers of YR may be linked to Hg speciation. In a previous study on YR, inorganic mercury (InHg) comprised a major proportion of the total Hg (mean = 58 ± 14.2%) in liver tissue (Barst et al. 2015). In addition to elevated proportions of InHg in the livers of YR, Barst et al. (2015) demonstrated a co-localization of Hg and Se within hepatic MA. The authors hypothesized that InHg was bound to Se, forming HgSe granules that are thought to be the end-product of MeHg detoxification (Wang et al. 2012). The accumulation of total Hg in the metal-rich granule fractions of YR may therefore represent a long-term accumulation of HgSe granules in YR livers. In the same manner, the low accumulation of total Hg in the metal-rich granule

fraction of Arctic char (Barst et al. 2016) and rabbitfish (Peng et al. 2016) may be a result of the low proportions of InHg in their tissues.

Despite the accumulation of total Hg in HSP and metal-rich granules, detoxification in the livers of YR was incomplete, as evidenced by the total Hg present in metal-sensitive fractions, and the increase in total Hg concentration in these fractions along the bioaccumulation gradient. The total Hg found in the sensitive fractions of YR liver could negatively impact the health of these fish. For example, Cambier et al. (2009) noted an inhibition of both state 3 mitochondrial respiration and cytochrome c oxidase activity in the muscle fibers of zebrafish exposed to an environmentally-relevant dose of dietary MeHg for 49 days. As the mitochondria fraction contributed the greatest percentage of total Hg among sensitive and detoxified fractions, YR could be suffering from inhibited respiration and thus, altered energy metabolism. The accumulation of total Hg in the HDP fraction could have consequences for the redox defense system; Se-dependent enzymes, such as glutathione peroxidase (GSH-Px) and thioredoxin reductase (TrxR), are likely molecular targets for intracellular Hg due to the high binding affinity Hg has for Se. In support of this, a laboratory feeding study documented decreased activity of GSH-Px in the brains of juvenile Atlantic salmon (*Salmo salar*) exposed to MeHg (Berntssen et al., 2003). Decreased activities of GSH-Px and TrxR have also been documented in the tissues of zebra-seabream (*Diplodus cervinus*) following aqueous exposure to either MeHg or InHg (Branco et al., 2012). As previously stated, the presence of total Hg in the microsomes and lysosomes fraction is more difficult to interpret, and our inability to classify this fraction in either the detoxified or sensitive compartment provides an opportunity for future studies.

4.6. Se (selenium)

In contrast to the other elements measured in YR livers, Se is essential to normal cellular function. Despite this essential nature, above a threshold concentration Se may become toxic. Given that the range of concentrations in YR livers in the present study is within the range of those reported to afford protection from oxidative stress in the livers of yellow perch (Ponton et al. 2016), we discuss Se in YR in

the context of its potential ameliorative effects. Selenium is known to have an interaction with non-essential metals such as Cd, As, and Hg (Sasakura and Suzuki, 1998), and this may confer a protective action against toxicity (Banni et al., 2011; Wang et al., 2013). We chose to include Se in the present study because it is known to have a strong binding affinity for Hg and it is well understood that Hg handling in the subcellular environment involves interactions with selenols (Wang et al. 2012). Additionally, previous work has demonstrated colocalization of Hg and Se in immune cells, suggesting an interaction between the two elements within YR livers (Barst et al. 2015). The protective effects of Se on Hg toxicity have been the subject of a significant amount of research, some of which hypothesizes that Se is protective if molar ratios (Se:Hg) meet or exceed unity (Ralston et al. 2007). However this protective effect has been largely studied from a human health perspective and has not been well explored in terms of the health of wild fish nor focused on the liver with its major role in detoxification. Within the detoxified compartment, Se was found primarily in the HSP fraction, and to a lesser extent in the granule-like fraction. Within the HSP fraction, Se is most likely present as seleno-cysteine (Gladyshev, 2012) in thermostable metal-binding proteins, such as MT. As previously mentioned, Se within the granule-like fraction may be present as HgSe. In contrast to Arctic char livers, where less than 2% of the total Se burden was associated with the metal-rich granule fraction, the granule-like fraction isolated from YR livers comprised an average of 10% of the total Se burden. Interestingly, the percentages of Se in the metal-rich granules isolated from both species of fish were similar to the proportions of total Hg in the respective fractions. This is likely another indication of the interaction between the two elements. The proportion of Se within the metal-sensitive compartment roughly equaled that in the detoxified compartment. In metal-sensitive fractions, Se demonstrated a slight preference for the HDP fraction, which is not surprising given selenium's biochemical role in enzymes, such as GSH-Px and TrxR.

4.7. Overall subcellular element partitioning

We noted clear differences in the partitioning of the trace elements As, Cd, Pb, Hg, and Se in the livers of YR. As Class B metals, Hg and Cd have high affinities for thiols in biological systems, and therefore

these non-essential metals would be expected to display similar subcellular partitioning. Both elements appear in the same quadrant in both PCA loading plots (bottom right) for the metal-sensitive and the detoxified metal compartments (Figure 5A-B), which presumably reflects the common affinity that these metals have for SH- functional groups. Conversely, both As and Pb are borderline elements, and their proximity within the PCA plots is likely a result of the lower affinities that these metals share for thiols relative to "soft" metals such as Cd and Hg (Figures 5A and 5B). Interestingly, for the detoxified-metal compartment, As and Hg vectors are directed in opposite directions (both vectors are projected at 180°) in the PCA figure, indicating a potential negative relationship between the partitioning of As and Hg in this compartment. A similar trend between As and Hg is also observed in the metal-sensitive compartment, where the metal vectors are projected perpendicularly. We speculate that both elements could be targeting similar biomolecules. Additionally, the location of the Se vector between the As and Hg vectors may indicate potential interactions between Se and these two elements.

Yelloweye rockfish were able to maintain some of these non-essential metals in detoxified fractions, suggesting an ability to cope with these metals to some extent. Both Cd and As were mainly found in the HSP fraction within the detoxified compartment, indicating a potential interaction with MT. In contrast, both Pb and Hg showed a greater preference for the granule-like fraction than the HSP fraction. For Pb, this trend is consistent with results from subcellular partitioning in eels (Rosabal et al. 2015), but for Hg this apparent role of the granule-like fraction within the livers of YR is not consistent with results of a previous study with Arctic char, in which the HSP played a much more important role in detoxification. We hypothesize that the observed divergence may be related to differences in Hg speciation and/or age between the two species of fish. Future studies should focus on exploring the subcellular partitioning of InHg and MeHg to determine possible differences.

Although, non-essential metals were associated with detoxified fractions within the livers of YR, detoxification was incomplete as each of the non-essential metals was also associated with potentially-sensitive sites. However, only Pb and Hg increased significantly within potentially-sensitive fractions along the bioaccumulation gradient, suggesting that within the tissue concentration ranges reported here

YR are less efficient at detoxifying these metals than Cd and As. Within the potentially-sensitive compartment, the fraction containing mitochondria was consistently important for binding of Cd, Pb, As, and Hg. The accumulation of these non-essential metals in this fraction may lead to negative effects, given the key role that these organelles play in cellular metabolism. Subcellular partitioning procedures, such as the one employed in the present work, provide useful information on how trace elements are distributed within cells, thus moving beyond more simple measures in bulk tissues. This type of information can be useful when trying to understand risk associated with multiple non-essential elements. Collectively, our results suggest that Hg may be of greatest concern to the health of YR relative to the other non-essential metals studied; the majority of Hg was associated with the sensitive compartment, whereas the other non-essential metals were predominately associated with the detoxified compartment. Recent analyses of the available data for Hg toxicity in fish indicate that toxic effects are likely to occur at concentrations exceeding 0.3 µg g^{-1} ww (Dillon et al. 2010; Sandheinrich and Wiener, 2011) (equivalent concentration in edible muscle 0.5 µg g^{-1} ww). In the present study, 5 of the 8 YR exceed this toxicity threshold (Table 1), suggesting that they are indeed at risk for the toxic effects of Hg. Our work demonstrates that non-essential metals accumulate in potentially-sensitive sites (mitochondria, microsomes, and enzymes), which may have implications for the health of YR.

Acknowledgements

We thank A. Caron, J. Perreault and R. Rodrigue for laboratory assistance. We also thank members of the Griggers family at TreeTops Lodge for lodging and assistance in the field. P.G.C. Campbell and N. Basu are supported by the Canada Research Chairs programme. This project was supported by the NSERC Discovery Grant programme (Drevnick).

Supplementary Information

Consists of methods related to subcellular partitioning and trace element analyses, in addition to three figures (S2, S3, and S4).

Table 1. Ranges in lengths and weights, mean hepatic trace element concentrations (nmol g^{-1} dw), and total mercury concentrations in muscle (µg g^{-1} ww) of yelloweye rockfish (*Sebastes ruberrimus*) collected in southeast Alaska.

			Liver concentrations (nmol g^{-1} dw)					Muscle concentrations (µg g^{-1} ww)
Fish	**Length (cm)**	**Weight (g)**	**As**	**Cd**	**Pb**	**Hg**	**Se**	**Hg**
1	64.5	4320	59.5	147.3	1.2	14.2	249.6	0.63
2	57.5	2530	74.8	116.7	1.0	13.7	241.3	0.29
3	54.8	3020	51.6	89.6	0.3	25.0	148.3	0.38
4	51.5	2140	148.7	53.5	0.7	9.8	136.8	0.30
5	57.0	2750	110.1	131.9	1.2	18.3	226.9	0.59
6	57.0	2640	77.4	105.1	0.6	10.7	279.5	0.51
7	62.3	3740	85.8	478.8	1.5	39.6	417.0	1.44
8	79.0	8800	64.5	90.4	0.4	22.7	202.7	0.88
n	8	8	23[a]	22[a]	18[a]	21[a]	23[a]	8
min	51.5	2140	51.6	53.5	0.3	9.8	136.8	0.3
max	79.0	8800	148.7	478.8	1.5	39.6	417.0	1.4
max:min	1.5	4.1	2.9	9.0	4.7	4.1	3.0	4.9

[a] n represents the total number of liver samples for which the mass balance recovery was between 61 and 150 %.

5. References

Araújo, O., Pereira, P., Cesário, R., Pacheco, M., Raimundo, J., 2015. The sub-cellular fate of mercury in the liver of wild mullets (*Liza aurata*)–Contribution to the understanding of metal-induced cellular toxicity. Mar. Pollut. Bull. 95, 412-418.

Banni, M., Chouchene, L., Said, K., Kerkeni, A., Messaoudi, I., 2011. Mechanisms underlying the protective effect of zinc and selenium against cadmium-induced oxidative stress in zebrafish *Danio rerio*. BioMetals 24, 981-992.

Barst, B.D., Bridges, K., Korbas, M., Roberts, A.P., Van Kirk, K., McNeel, K., Drevnick, P.E., 2015. The role of melano□macrophage aggregates in the storage of mercury and other metals: An example from yelloweye rockfish (*Sebastes ruberrimus*). Environ. Toxicol. Chem. 34, 1918-1925.

Barst, B.D., Rosabal, M., Campbell, P.G., Muir, D.G., Wang, X., Köck, G., Drevnick, P.E., 2016. Subcellular distribution of trace elements and liver histology of landlocked Arctic char (*Salvelinus alpinus*) sampled along a mercury contamination gradient. Environ. Pollut. 212, 574-583.

Béchard, K., Gillis, P., Wood, C., 2008. Trophic transfer of Cd from larval chironomids (Chironomus riparius) exposed via sediment or waterborne routes, to zebrafish (*Danio rerio*): Tissue-specific and subcellular comparisons. Aquat. Toxicol. 90, 310-321.

Berntssen, M., Aatland, A., Handy, R., 2003. Chronic dietary mercury exposure causes oxidative stress, brain lesions, and altered behaviour in Atlantic salmon (*Salmo salar*) parr. Aquat. Toxicol. 65, 55-72.

Branco, V., Canário, J., Lu, J., Holmgren, A., Carvalho, C., 2012. Mercury and selenium interaction in vivo: effects on thioredoxin reductase and glutathione peroxidase. Free Radical Biol. Med. 52, 781-793.

Cambier, S., Benard, G., Mesmer-Dudons, N., Gonzalez, P., Rossignol, R., Brethes, D., Bourdineaud, J.-P., 2009. At environmental doses, dietary methylmercury inhibits mitochondrial

energy metabolism in skeletal muscles of the zebra fish (*Danio rerio*). The international journal of biochemistry & cell biology 41, 791-799.

Campbell, P.G., Hare, L., 2009. Metal detoxification in freshwater animals. Roles of metallothioneins. Metallothioneins and related chelators, 239-277.

Caron, A., Rosabal, M., Drevet, O., Couture, P., Campbell, P.G., 2018. Binding of trace elements (Ag, Cd, Co, Cu, Ni, and Tl) to cytosolic biomolecules in livers of juvenile yellow perch (Perca flavescens) collected from lakes representing metal contamination gradients. Environmental Toxicology and Chemistry 37, 576-586.

COSEWIC, 2009. COSEWIC assessment and status report on the Yelloweye rockfish, *Sebastes ruberrimus*: Pacific Ocean inside waters population, Pacific Ocean outside waters population in Canada.

Couture, P., Pyle, G., 2008. Live fast and die young: metal effects on condition and physiology of wild yellow perch from along two metal contamination gradients. Hum. Ecol. Risk Assess. 14, 73-96.

Couture, P., Rajotte, J.W., 2003. Morphometric and metabolic indicators of metal stress in wild yellow perch (*Perca flavescens*) from Sudbury, Ontario: a review. J. Environ. Monit. 5, 216-221.

Dang, F., Rainbow, P.S., Wang, W.-X., 2012. Dietary toxicity of field-contaminated invertebrates to marine fish: Effects of metal doses and subcellular metal distribution. Aquat. Toxicol. 120, 1-10.

Dillon, T., Beckvar, N., Kern, J., 2010. Residue based mercury dose–response in fish: An analysis using lethality equivalent test endpoints. Environ. Toxicol. Chem. 29, 2559-2565.

Giguère, A., Campbell, P.G., Hare, L., Couture, P., 2006. Sub-cellular partitioning of cadmium, copper, nickel and zinc in indigenous yellow perch (*Perca flavescens*) sampled along a polymetallic gradient. Aquat. Toxicol. 77, 178-189.

Gladyshev, V.N., 2012. Selenoproteins and selenoproteomes, Selenium. Springer, pp. 109-123.

Goto, D., Wallace, W.G., 2010. Metal intracellular partitioning as a detoxification mechanism for mummichogs (*Fundulus heteroclitus*) living in metal-polluted salt marshes. Mar. Environ. Res. 69, 163-171.

He, M., Ke, C.-H., Wang, W.-X., 2010. Effects of cooking and subcellular distribution on the bioaccessibility of trace elements in two marine fish species. J. Agric. Food Chem. 58, 3517-3523.

Hinton, R.H., Mullock, B.M., Gilhuus-Moe, C., 1997. Isolation of subcellular fractions. Subcellular Fractionation: A Practical Approach, 31-69.

Luoma, S.N., Rainbow, P.S., 2005. Why is metal bioaccumulation so variable? Biodynamics as a unifying concept. Environmental Science & Technology 39, 1921-193

Love, M.S., Yoklavich, M., Thorsteinson, L.K., 2002. The rockfishes of the northeast Pacific. Univ of California Press.

Marigómez, I., Soto, M., Cajaraville, M.P., Angulo, E., Giamberini, L., 2002. Cellular and subcellular distribution of metals in molluscs. Microsc. Res. Tech. 56, 358-392.

Mason, A., Jenkins, K., 1995. Metal detoxification in aquatic organisms. Metal speciation and bioavailability in aquatic systems 3, 479-608.

Müller, A.-K., Brinkmann, M., Baumann, L., Stoffel, M.H., Segner, H., Kidd, K.A., Hollert, H., 2015. Morphological alterations in the liver of yellow perch (*Perca flavescens*) from a biological mercury hotspot. Environmental Science and Pollution Research, 1-13.

Khan, M.A.K., Wang, F., 2009. Mercury selenium compounds and their toxicological significance: Toward a molecular understanding of the mercury selenium antagonism. Environ. Toxicol. Chem. 28, 1567-1577.

Korbas, M., O'Donoghue, J.L., Watson, G.E., Pickering, I.J., Singh, S.P., Myers, G.J., Clarkson, T.W., George, G.N., 2010. The chemical nature of mercury in human brain following poisoning or environmental exposure. ACS chemical neuroscience 1, 810-818.

Ng, T.Y.-T., Wood, C.M., 2008. Trophic transfer and dietary toxicity of Cd from the oligochaete to the rainbow trout. Aquat. Toxicol. 87, 47-59.

NMFS, 2010. Endangered and threatened wildlife and plants: threatened status for the Puget Sound/Georgia Basin distinct population segments of yelloweye and canary rockfish and endangered status for the Puget Sound/Georgia Basin distinct population segment of boccaccio rockfish, Final Rule. Federal Register, pp. 22276–22290.

Olsson, P.E., Hogstrand, C., 1987. Subcellular distribution and binding of cadmium to metallothionein in tissues of rainbow trout after exposure to 109Cd in water. Environ. Toxicol. Chem. 6, 867-874.

Palmisano, F., Cardellicchio, N., Zambonin, P., 1995. Speciation of mercury in dolphin liver: a two-stage mechanism for the demethylation accumulation process and role of selenium. Mar. Environ. Res. 40, 109-121.

Peng, X., Liu, F., Wang, W.X., 2016. Organ□specific accumulation, transportation and elimination of methylmercury and inorganic mercury in a low Hg accumulating fish. Environ. Toxicol. Chem.

Ponton, D.E., Caron, A., Hare, L., Campbell, P.G., 2016. Hepatic oxidative stress and metal subcellular partitioning are affected by selenium exposure in wild yellow perch (*Perca flavescens*). Environ. Pollut. 214, 608-617.

Ralston, N.V., Blackwell, J.L., Raymond, L.J., 2007. Importance of molar ratios in selenium-dependent protection against methylmercury toxicity. Biological Trace Element Research 119, 255-268.

Rogers, J., Richards, J., Wood, C., 2003. Ionoregulatory disruption as the acute toxic mechanism for lead in the rainbow trout (*Oncorhynchus mykiss*). Aquat. Toxicol. 64, 215-234.

Rosabal, M., Hare, L., Campbell, P.G., 2012. Subcellular metal partitioning in larvae of the insect *Chaoborus* collected along an environmental metal exposure gradient (Cd, Cu, Ni and Zn). Aquat. Toxicol. 120, 67-78.

Rosabal, M., Hare, L., Campbell, P.G., 2014. Assessment of a subcellular metal partitioning protocol for aquatic invertebrates: preservation, homogenization, and subcellular fractionation. Limnol. Oceanogr. Methods 12, 507-518.

Rosabal, M., Mounicou, S., Hare, L., Campbell, P.G.C., 2016. Metal (Ag, Cd, Cu, Ni, Tl, Zn) binding to cytosolic biomolecules in field-collected larvae of the insect *Chaoborus*. Environ. Sci. Technol. 50, 3247-3255.

Rosabal, M., Pierron, F., Couture, P., Baudrimont, M., Hare, L., Campbell, P.G., 2015. Subcellular partitioning of non-essential trace metals (Ag, As, Cd, Ni, Pb, and Tl) in livers of American (*Anguilla rostrata*) and European (*Anguilla anguilla*) yellow eels. Aquat. Toxicol. 160, 128-141.

Sánchez-Marín, P., Beiras, R., 2017. Subcellular distribution and trophic transfer of Pb from bivalves to the common prawn *Palaemon serratus*. Ecotoxicol. Environ. Saf. 138, 253-259.

Sandheinrich, M., Wiener, J., 2011. Methylmercury in freshwater fish: recent advances in assessing toxicity of environmentally relevant exposures. Environmental Contaminants in Biota: Interpreting Tissue Concentrations 2, 169-190.

Sasakura, C., Suzuki, K.T., 1998. Biological interaction between transition metals (Ag, Cd and Hg), selenide/sulfide and selenoprotein P. Journal of inorganic biochemistry 71, 159-162.

US Environmental Protection Agency, 2007. Method 7473: Mercury in solids and solutions by thermal decomposition, amalgamation, and atomic absorption spectrophotometry, Washington, D.C.

Wallace, W.G., Lee, B.-G., Luoma, S.N., 2003. Subcellular compartmentalization of Cd and Zn in two bivalves. I. Significance of metal-sensitive fractions (MSF) and biologically detoxified metal (BDM). Mar. Ecol. Prog. Ser. 249, 183-197.

Wang, Z., Feng, C., Ye, C., Wang, Y., Yan, C., Li, R., Yan, Y., Chi, Q., 2016. Subcellular partitioning profiles and metallothionein levels in indigenous clams *Moerella iridescens* from a metal-impacted coastal bay. Aquat. Toxicol. 176, 10-23.

Wang, F., Lemes, M., Khan, M., 2012. Metallomics of mercury: Role of thiol-and selenol-containing biomolecules. Environmental Chemistry and Toxicology of Mercury, 517.

Wang, Y., Wu, Y., Luo, K., Liu, Y., Zhou, M., Yan, S., Shi, H., Cai, Y., 2013. The protective effects of selenium on cadmium-induced oxidative stress and apoptosis via mitochondria pathway in mice kidney. Food Chem. Toxicol. 58, 61-67.

Watanabe, T., Hirano, S., 2013. Metabolism of arsenic and its toxicological relevance. Arch. Toxicol. 87, 969-979.

Wolke, R., 1992. Piscine macrophage aggregates: a review. Annu. Rev. Fish Dis. 2, 91-108.

Zhang, W., Huang, L., Wang, W.-X., 2012. Biotransformation and detoxification of inorganic arsenic in a marine juvenile fish *Terapon jarbua* after waterborne and dietborne exposure. J. Hazard. Mater. 221, 162-169.

Zhang, L., Wang, W.-X., 2006. Significance of subcellular metal distribution in prey in influencing the trophic transfer of metals in a marine fish. Limnol. Oceanogr. 51, 2008-2017.

Figure Captions

Figure 1. Relationships between total hepatic trace element concentration (x-axes) and trace element concentrations in subcellular fractions (y-axes) isolated from the livers of yelloweye rockfish (*Sebastes ruberrimus*). Upper panels (A, C, E) represent sensitive fractions and the lower panels (B, D, F) represent detoxified fractions. The various subcellular fractions are: mitochondria (filled triangles), microsomes and lysosomes (white triangles), heat-denatured proteins (white stars), heat-stable proteins (white squares), and granule-like (black squares). Points represent means of replicate livers and error bars represent standard deviations. Lines represent statistically significant regressions ($P < 0.05$). Points in boxes are outliers and were excluded from regressions.

Figure 2. Mean relative contributions of cadmium (Cd), and lead (Pb) in various subcellular fractions isolated from the livers of yelloweye rockfish (*Sebastes ruberrimus*). Subcellular fraction abbreviations are: MITO = mitochondria, M+L = microsomes and lysosomes, HDP = heat-denatured proteins, DEB = debris and nuclei, HSP = heat-stable proteins, and GRAN = granule-like. Note that arsenic (As) data are not presented as the relative proportions of As varied significantly in both the HSP and M+L fractions along the bioaccumulation gradient.

Figure 3. Relationships between total hepatic trace element concentration (x-axes) and trace element concentrations in subcellular fractions (y-axes) isolated from the livers of yelloweye rockfish (*Sebastes ruberrimus*). Upper panels (G and I) represent sensitive fractions and the lower panels (H and J) represent detoxified fractions. The various subcellular fractions are: mitochondria (filled triangles), microsomes and lysosomes (white triangles), heat-denatured proteins (white stars), heat-stable proteins (white squares), and granule-like (black squares). Points represent means of replicate livers and error bars represent standard deviations. Lines represent statistically significant

regressions ($P < 0.05$). Points in boxes are outliers and were excluded from regressions.

Figure 4. Mean relative contributions of mercury (Hg) and selenium (Se) in various subcellular fractions isolated from the livers of yelloweye rockfish (*Sebastes ruberrimus*). Subcellular fraction abbreviations are: MITO = mitochondria, M+L = microsomes and lysosomes, HDP = heat-denatured proteins, DEB = debris and nuclei, HSP = heat-stable proteins, and GRAN = granule-like.

Figure 5. Principal Component Analysis (PCA) based on trace element concentrations in sensitive (A) and detoxified (B) fractions isolated from the livers of yelloweye rockfish (*Sebastes ruberrimus*).

Figure S1. Flow chart describing the partitioning procedure used to separate yelloweye rockfish livers into subcellular fractions.

Figure S2. Relationships between total hepatic trace element concentration (x-axes) and relative contributions of subcellular fractions (y-axes) isolated from the livers of yelloweye rockfish (*Sebastes ruberrimus*). Upper panels (A, C, E) represent sensitive fractions and the lower panels (B, D, F) represent detoxified fractions. The various subcellular fractions are: mitochondria (filled triangles), microsomes and lysosomes (white triangles), heat-denatured proteins (white stars), heat-stable proteins (white squares), and granule-like (black squares). Points represent means of replicate livers and error bars represent standard deviations. Lines represent statistically significant regressions ($P < 0.05$). Points in boxes are outliers and were excluded from regressions.

Figure S3. Relationships between total hepatic trace element concentration (x-axes) and the relative contributions of subcellular fractions (y-axes) isolated from the livers of yelloweye rockfish (*Sebastes ruberrimus*). Upper panels (A, C) represent sensitive fractions and the lower panels (B, D) represent detoxified fractions. The various subcellular fractions are: mitochondria (filled triangles), microsomes and lysosomes

(white triangles), heat-denatured proteins (white stars), heat-stable proteins (white squares), and granule-like (black squares). Points represent means of replicate livers and error bars represent standard deviations. Points in boxes are outliers and were excluded from regressions.

Figure 1. Relationships between total hepatic trace element concentration (x-axes) and trace element concentrations in subcellular fractions (y-axes) isolated from the livers of yelloweye rockfish (*Sebastes ruberrimus*). Upper panels (A, C, E) represent sensitive fractions and the lower panels (B, D, F) represent detoxified fractions. The various subcellular fractions are: mitochondria (filled triangles), microsomes and lysosomes (white triangles), heat-denatured proteins (white stars), heat-stable proteins (white squares), and granule-like (black squares). Points represent means of replicate livers and error bars represent standard deviations. Lines represent statistically significant regressions ($P < 0.05$). Points in boxes are outliers and were excluded from regressions.

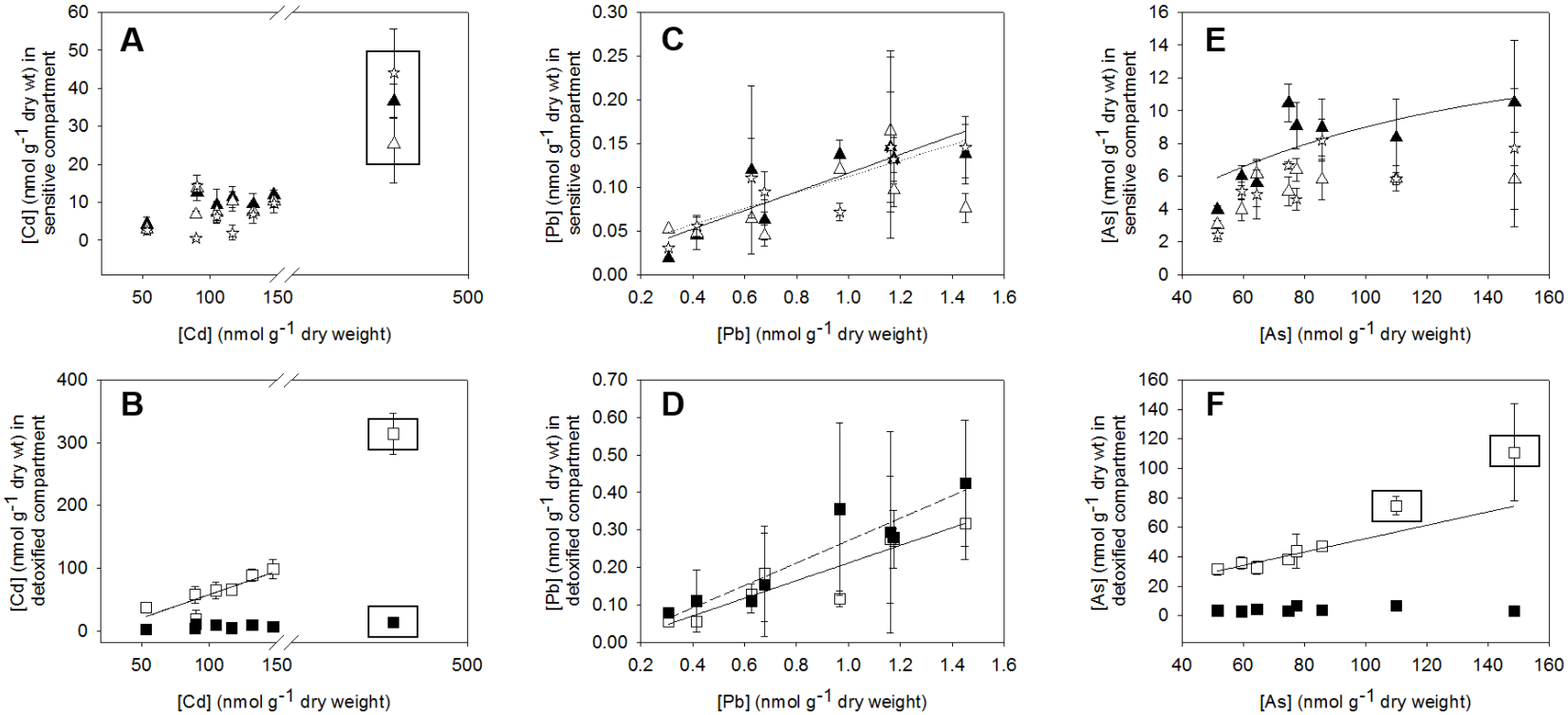

Figure 2. Mean relative contributions of cadmium (Cd), and lead (Pb) in various subcellular fractions isolated from the livers of yelloweye rockfish (*Sebastes ruberrimus*). Subcellular fraction abbreviations are: MITO = mitochondria, M+L = microsomes and lysosomes, HDP = heat-denatured proteins, DEB = debris and nuclei, HSP = heat-stable proteins, and GRAN = granule-like. Note that arsenic (As) data are not presented as the relative proportions of As varied significantly in both the HSP and M+L fractions along the bioaccumulation gradient.

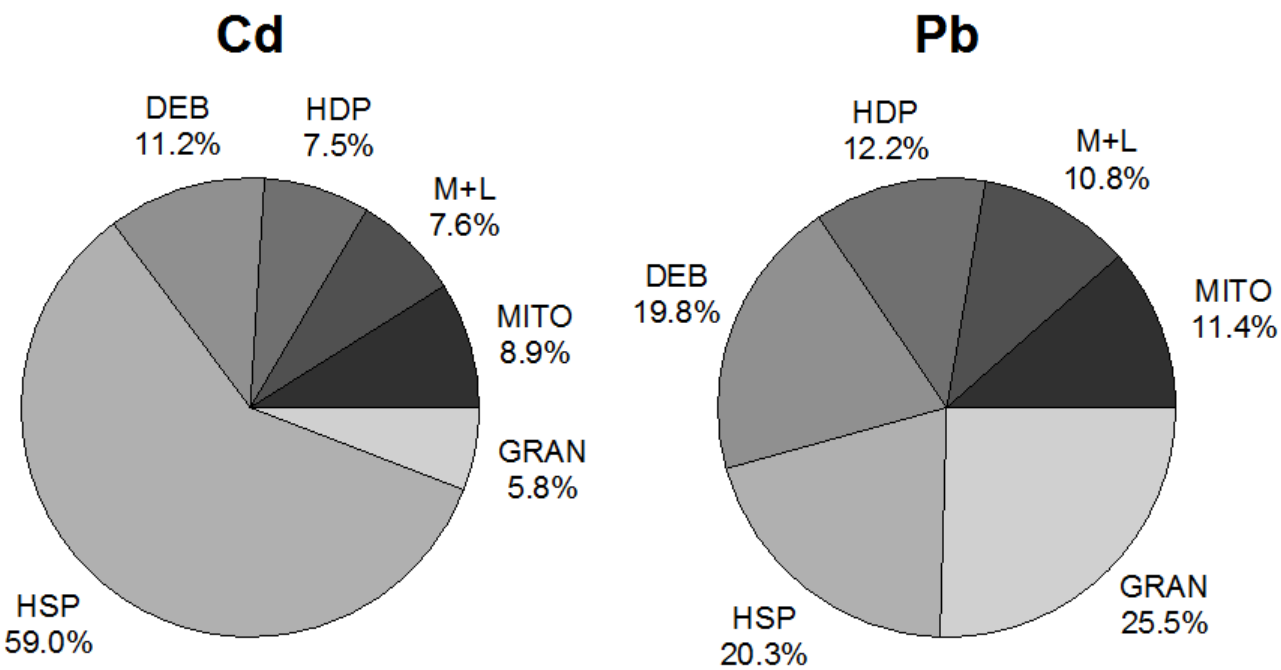

Figure 3. Relationships between total hepatic trace element concentration (x-axes) and trace element concentrations in subcellular fractions (y-axes) isolated from the livers of yelloweye rockfish (*Sebastes ruberrimus*). Upper panels (G and I) represent sensitive fractions and the lower panels (H and J) represent detoxified fractions. The various subcellular fractions are: mitochondria (filled triangles), microsomes and lysosomes (white triangles), heat-denatured proteins (white stars), heat-stable proteins (white squares), and granule-like (black squares). Points represent means of replicate livers and error bars represent standard deviations. Lines represent statistically significant regressions ($P < 0.05$). Points in boxes are outliers and were excluded from regressions.

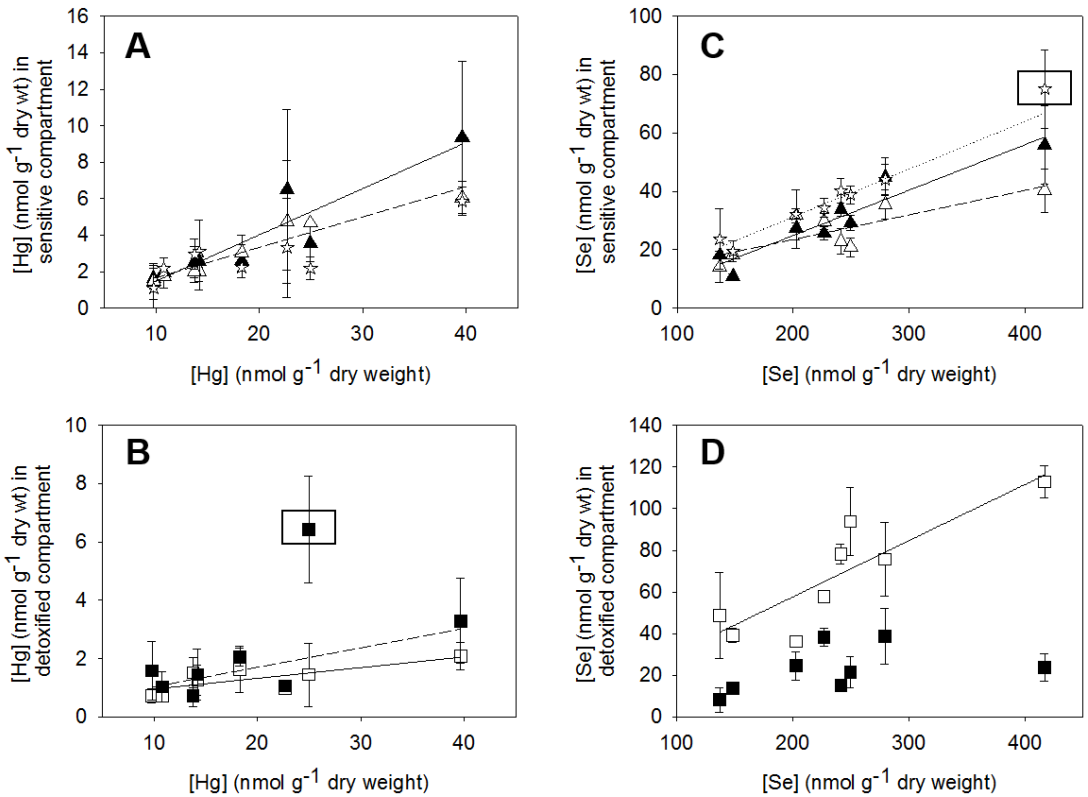

Figure 4. Mean relative contributions of mercury (Hg) and selenium (Se) in various subcellular fractions isolated from the livers of yelloweye rockfish (*Sebastes ruberrimus*). Subcellular fraction abbreviations are: MITO = mitochondria, M+L = microsomes and lysosomes, HDP = heat-denatured proteins, DEB = debris and nuclei, HSP = heat-stable proteins, and GRAN = granule-like.

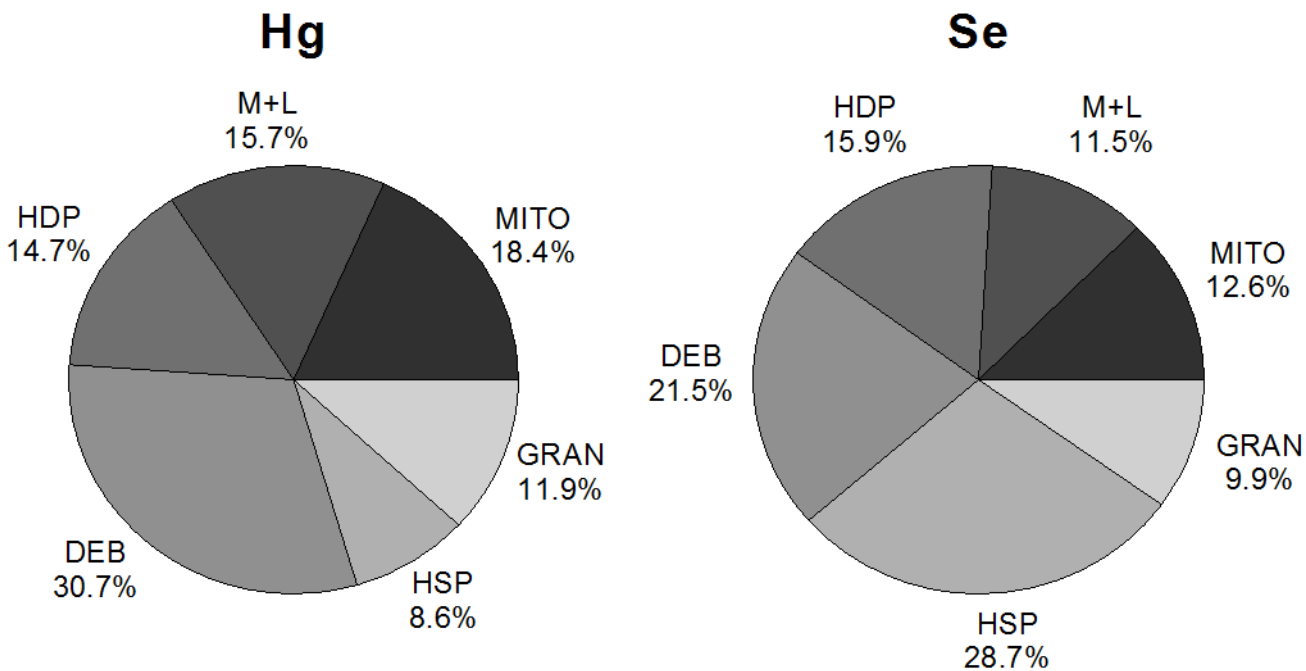

Figure 5. Principal Component Analysis (PCA) based on trace element concentrations in sensitive (A) and detoxified (B) fractions isolated from the livers of yelloweye rockfish (*Sebastes ruberrimus*).

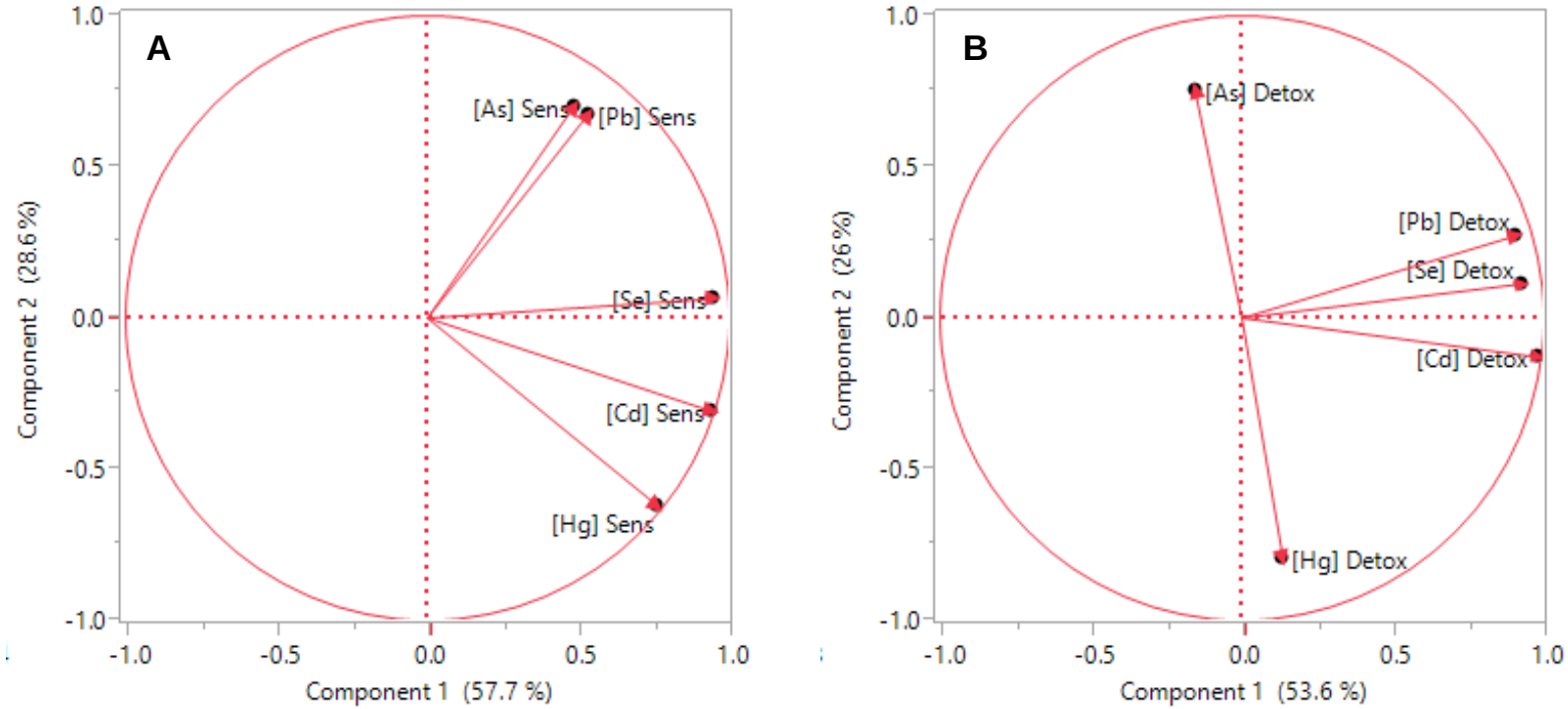

Figure S1. Flow chart describing the partitioning procedure used to separate yelloweye rockfish livers into subcellular fractions.

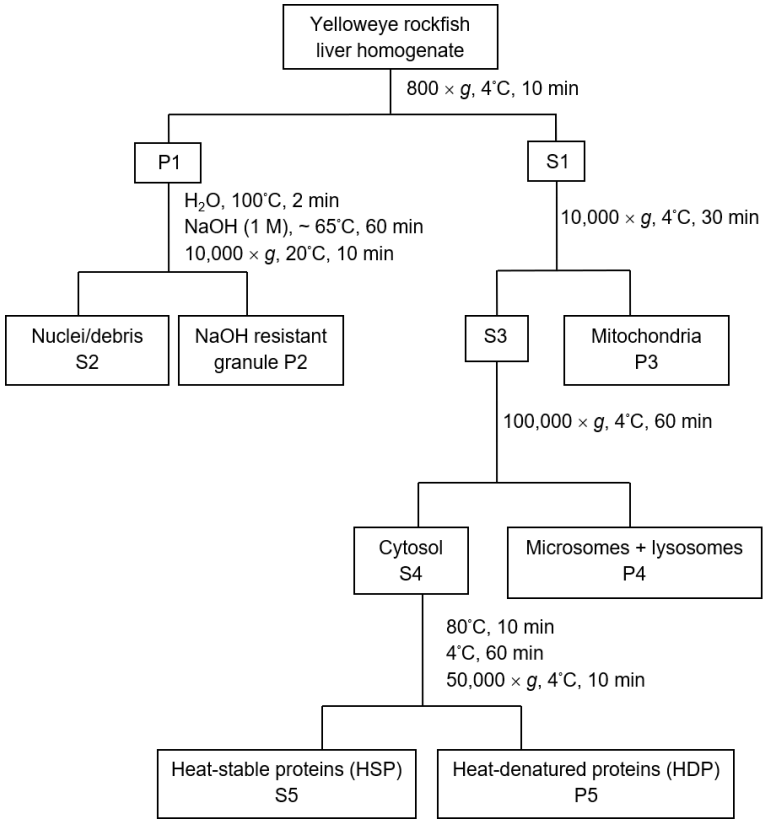

Figure S2. Relationships between total hepatic trace element concentration (x-axes) and relative contributions of subcellular fractions (y-axes) isolated from the livers of yelloweye rockfish (*Sebastes ruberrimus*). Upper panels (A, C, E) represent sensitive fractions and the lower panels (B, D, F) represent detoxified fractions. The various subcellular fractions are: mitochondria (filled triangles), microsomes and lysosomes (white triangles), heat-denatured proteins (white stars), heat-stable proteins (white squares), and granule-like (black squares). Points represent means of replicate livers and error bars represent standard deviations. Lines represent statistically significant regressions ($P < 0.05$). Points in boxes are outliers and were excluded from regressions.

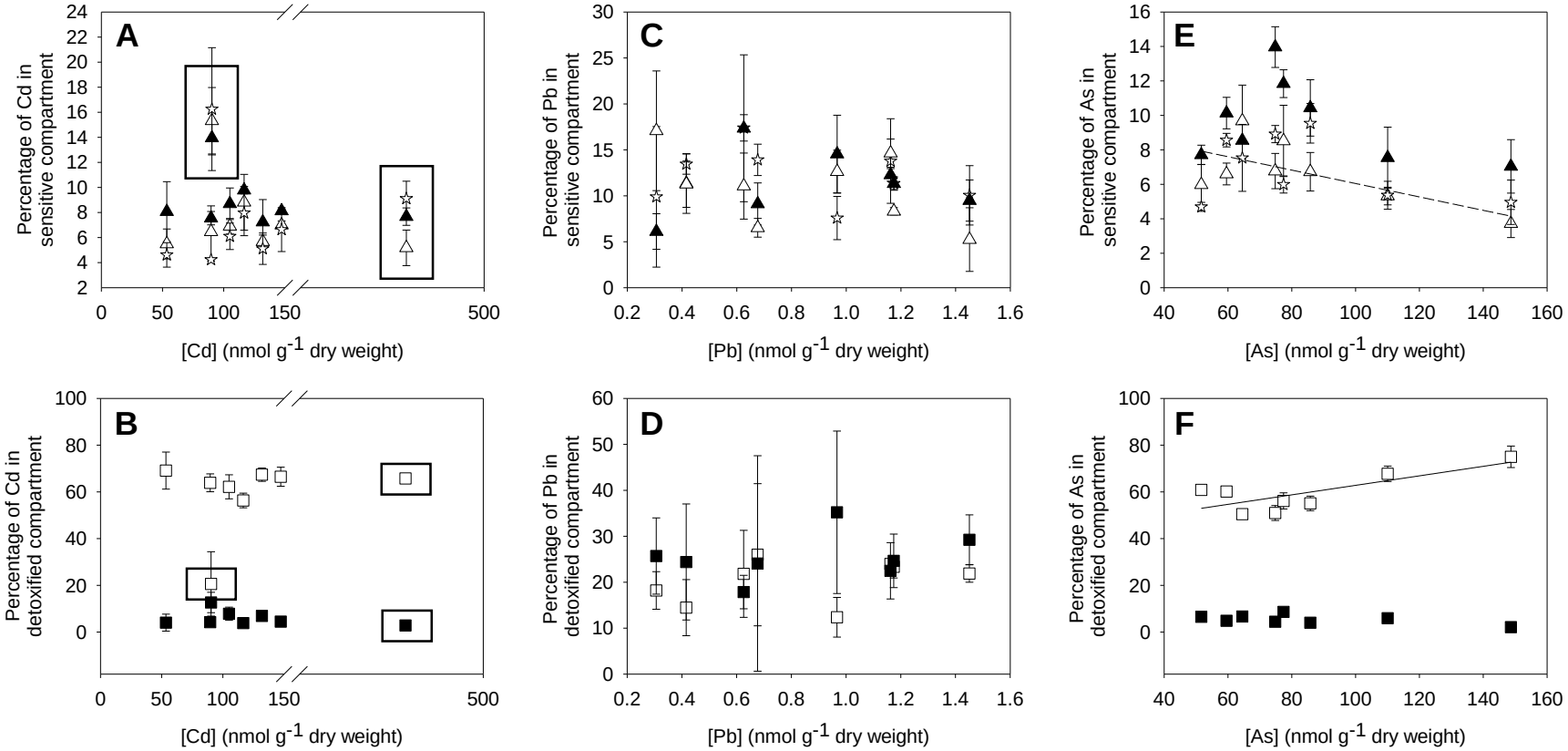

Figure S3. Relationships between total hepatic trace element concentration (x-axes) and the relative contributions of subcellular fractions (y-axes) isolated from the livers of yelloweye rockfish (*Sebastes ruberrimus*). Upper panels (A, C) represent sensitive fractions and the lower panels (B, D) represent detoxified fractions. The various subcellular fractions are: mitochondria (filled triangles), microsomes and lysosomes (white triangles), heat-denatured proteins (white stars), heat-stable proteins (white squares), and granule-like (black squares). Points represent means of replicate livers and error bars represent standard deviations. Points in boxes are outliers and were excluded from regressions.

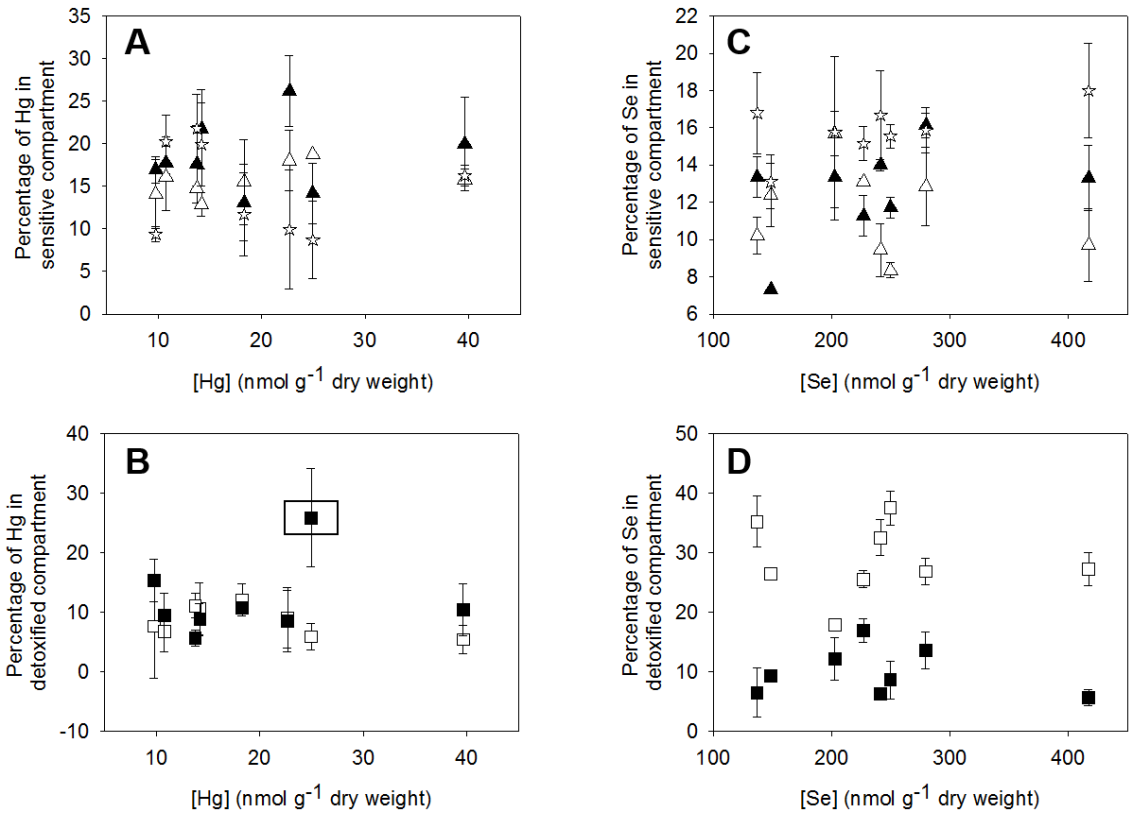

Highlights

- Subcellular partitioning of Cd, Pb, As, Hg, and Se was determined in the livers of yelloweye rockfish.
- Though non-essential elements were found in detoxified fractions, the extent of binding differed among elements.
- Mercury may be of particular concern, as it was present mainly in sensitive sites.